Hydrogen Tunneling and Protein Motion in Enzyme Reactions

SHARON HAMMES-SCHIFFER

Department of Chemistry, 104 Chemistry Building,
Pennsylvania State University,
University Park, Pennsylvania 16802

ABSTRACT
Theoretical perspectives on hydrogen transfer reactions in enzymes are presented. The proton-coupled electron transfer reaction catalyzed by soybean lipoxygenase and the hydride transfer reaction catalyzed by dihydrofolate reductase are discussed. The first reaction is nonadiabatic and involves two distinct electronic states, while the second reaction is predominantly adiabatic and occurs on the electronic ground state. Theoretical studies indicate that hydrogen tunneling and protein motion play significant roles in both reactions. In both cases, the proton donor−acceptor distance decreases relative to its equilibrium value to enable efficient hydrogen tunneling. Equilibrium thermal motions of the protein lead to conformational changes that facilitate hydrogen transfer, but the nonequilibrium dynamical aspects of these motions have negligible impact.

Introduction

Hydrogen transfer reactions play a vital role in a wide range of enzymatic reactions. Theoretical studies of hydrogen transfer reactions in enzymes have provided insight into biologically significant issues. Modern computational methods have enabled the calculation of rates and kinetic isotope effects (KIEs) for comparison to experiment and to make predictions that can be tested experimentally.[1−3] Recent computer simulations have elucidated the fundamental nature of hydrogen nuclear quantum effects, including zero point energy, hydrogen tunneling, and excited vibrational states. Theoretical studies have also enhanced our understanding of the role of the structure and motion of enzymes and the impact of mutations on enzyme catalysis.

Nuclear quantum effects such as hydrogen tunneling are significant in hydrogen transfer reactions due to the light mass of hydrogen. A variety of approaches have been developed to include the nuclear quantum effects in simulations of enzymatic reactions. In mixed quantum/classical methods, the transferring hydrogen nucleus is represented as a vibrational wave function, analogous to electronic wave functions, while the remaining nuclei are treated classically.[4,5] Theoretical formulations have been developed for both adiabatic reactions,[6] which occur on the ground state, and nonadiabatic reactions,[5,7] which involve multiple electronic or vibrational states. Both types of reactions have been observed in enzyme catalysis.

Protein motion can impact enzymatic reactions in numerous ways.[2,8−16] For example, enzyme motion can affect the activation free energy barrier for the reaction. The free energy is related to the probability of obtaining configurations with a specified value of the reaction coordinate, where higher free energy corresponds to lower probability. The transition state conformations, which correspond to relatively high free energy, are sampled infrequently. Enzyme motion can significantly impact the sampling of these relatively low-probability transition state configurations and thereby alter the free energy barrier. In addition, enzyme motion can influence the dynamical recrossings of the free energy barrier and the hydrogen tunneling probability.[1,2]

This Account summarizes the results of recent theoretical studies of two enzyme reactions involving hydrogen transfer. These enzymes were chosen based on their biochemical importance as well as the availability of experimental data. The first enzyme reaction is proton-coupled electron transfer (PCET) catalyzed by soybean lipoxygenase. This reaction is nonadiabatic and involves two distinct electronic states. The second enzyme reaction is hydride transfer catalyzed by dihydrofolate reductase. This reaction is predominantly adiabatic and occurs on the electronic ground state. The experimentally measured KIE (i.e., the ratio of the rate with hydrogen to the rate with deuterium) is ∼80 for soybean lipoxygenase[17] and ∼3 for dihydrofolate reductase[16,18] at room temperature. Theoretical and experimental studies indicate that hydrogen tunneling and protein motion play significant roles in both reactions.

Soybean Lipoxygenase

Lipoxygenases catalyze the oxidation of unsaturated fatty acids and have a wide range of biomedical applications.[19] Our calculations focused on soybean lipoxygenase (SLO), which catalyzes the net hydrogen atom transfer from a linoleic acid substrate to an iron cofactor, as depicted in Figure 1. This reaction occurs by a PCET mechanism, where the electron and proton transfer simultaneously between distinct donors and acceptors.[20,21] The PCET mechanism is supported by both computational and experimental results. Electronic structure calculations indicate that the electron transfers from an orbital on the substrate backbone to an orbital on the iron.[22] Moreover, a thermodynamic analysis based on electrochemical data indicates that the single proton and electron transfer reactions are highly endothermic by 30−40 kcal/mol, whereas the PCET reaction is slightly exothermic by ∼5 kcal/mol.[17,23] The PCET mechanism avoids these high-energy intermediates. This reaction is nonadiabatic due

Sharon Hammes-Schiffer received her B.A. from Princeton University in 1988 and her Ph.D. from Stanford University in 1993. After obtaining her Ph.D., she spent two years at AT&T Bell Laboratories as a postdoctoral research scientist. In 1995, she accepted a position as the Clare Boothe Luce Assistant Professor of Chemistry and Biochemistry at the University of Notre Dame. She moved to The Pennsylvania State University as the Shaffer Associate Professor of Chemistry in 2000 and was promoted to Professor of Chemistry in 2003. In 2001, she was appointed a Senior Editor of *The Journal of Physical Chemistry*. Her research centers on the theoretical and computational investigation of proton, hydride, and proton-coupled electron transfer reactions.
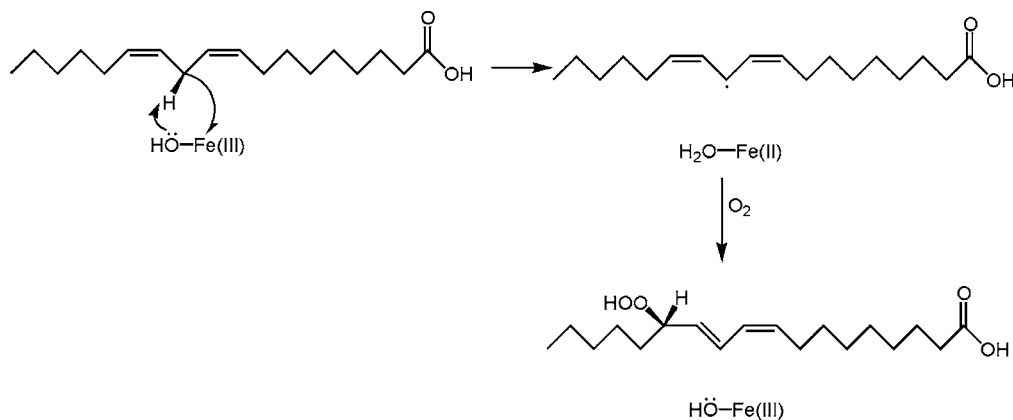
FIGURE 1. Proposed mechanism of soybean lipoxygenase. The calculations focus on the first step, which involves the net hydrogen atom transfer from the linoleic acid substrate to the Fe(III)—OH cofactor. Reproduced with permission from ref 23. Copyright 2004 American Chemcal Society.
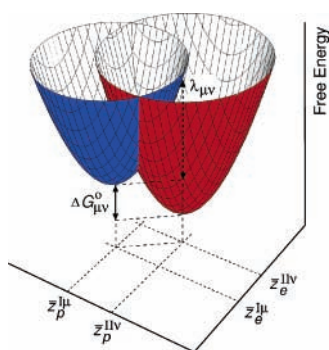
FIGURE 2. Two-dimensional vibronic free energy surfaces as functions of two collective solvent coordinates for a PCET reaction. The lowest energy reactant and product free energy surfaces are shown. The free energy difference, $\Delta G_{\mu\nu}^{\circ}$, and outer-sphere reorganization energy, $\lambda_{\mu\nu}$, are indicated.

to relatively small couplings between the reactant and product vibronic states. A number of theoretical approaches have been used to study this reaction.[17,22−25]

We have developed a general theoretical formulation for PCET reactions.[26,27] In this theory, the solute is represented by a four-state valence bond model corresponding to the four possible charge transfer states. The hydrogen nucleus is represented by a quantum mechanical wave function, and the solvent or protein environment can be described with a dielectric continuum model or with explicit molecules. We have shown that the free energy surfaces depend on two collective solvent coordinates corresponding to proton and electron transfer, and we have derived analytical expressions for these free energy surfaces.[26,27] The reactant and product electron−proton vibronic surfaces can be calculated as functions of the two solvent coordinates, as depicted in Figure 2. The reactant states correspond to the localization of the transferring electron on its donor, and the product states correspond to the localization of the transferring electron on its acceptor. Typically PCET reactions are nonadiabatic due to relatively small couplings between the reactant and product vibronic states. We have derived rate expressions for nonadiabatic PCET reactions using the Golden rule formalism. The PCET rate constant is the sum of the rate

constants for nonadiabatic transitions between all pairs of reactant and product vibronic states:

$$k = \frac{2\pi}{\hbar} \sum_{\mu}^{\{I\}} P_{\mu}^{I} \sum_{\nu}^{\{II\}} |V_{\mu\nu}|^2 (4\pi\lambda_{\mu\nu}k_{\mathrm{B}}T)^{-1/2} \exp\left(\frac{-(\Delta G_{\mu\nu}^{\circ} + \lambda_{\mu\nu})^2}{4\lambda_{\mu\nu}k_{\mathrm{B}}T}\right) \tag{1}$$

where the summations are over the reactant and product vibronic states, P_{μ}^{I} is the Boltzmann probability for the reactant state, $V_{\mu\nu}$ is the coupling between the reactant and product vibronic states, $\Delta G_{\mu\nu}^{\circ}$ is the free energy of reaction, and $\lambda_{\mu\nu}$ is the outer-sphere reorganization energy. The latter two quantities are depicted in Figure 2.

The implementation of this theory requires two types of input quantities. The gas phase empirical valence bond (EVB) matrix elements for the four-state VB model are represented by standard molecular mechanical terms that are parametrized to fit electronic structure calculations and experimental data.[3] The solvent/protein reorganization energy matrix elements are calculated with electrostatic dielectric continuum models. These quantities are used as input for the analytical expressions describing the reactant and product electronic free energy surfaces. Subsequently, the hydrogen vibrational wave functions are calculated for the reactant and product surfaces, leading to two sets of electron−proton vibronic surfaces. These surfaces provide the reorganization energies, free energies of reaction, and couplings, which are utilized in eq 1 to calculate the PCET rate constant. We have applied this formulation to a variety of PCET reactions in solution and have reproduced trends in rates and kinetic isotope effects, as well as the temperature and pH dependence in some cases.[28]

Recently, we used this theoretical formulation to study PCET in lipoxygenase.[23] The inner-sphere reorganization energy of the iron cofactor was determined to be ∼19 kcal/mol from density functional theory calculations on a model system. The outer-sphere reorganization energy of the protein was calculated to be ∼2.5 kcal/mol with an electrostatic dielectric continuum model for conformations obtained from docking simulations. The total reorganization energy was estimated to be the sum of these
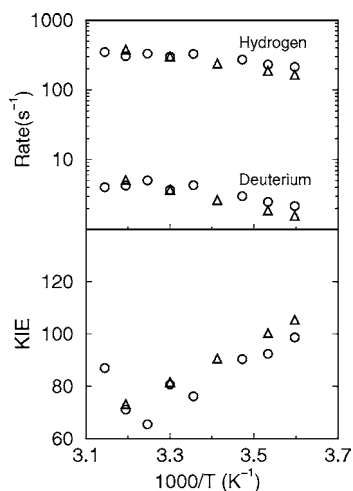
FIGURE 3. Temperature dependence of the rates and KIEs for the PCET reaction catalyzed by soybean lipoxygenase. The theoretical results[23] are denoted with open triangles, and the experimental data[17] are denoted with open circles. Reproduced with permission from ref 23. Copyright 2004 American Chemcal Society.
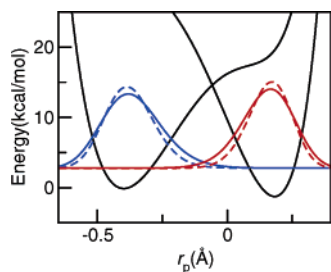
FIGURE 4. Reactant (blue) and product (red) proton potential energy curves and the associated hydrogen (solid) and deuterium (dashed) vibrational wave functions for the lowest energy reactant and product states for the PCET reaction catalyzed by SLO.[23]

inner-sphere and outer-sphere components. The gas phase EVB matrix elements were represented by standard molecular mechanical terms. The relative energies of the diabatic states were fit to electrochemical data, and the ET and PT couplings were fit to the experimental rate and KIE at 303 K.

As shown in Figure 3, the calculations reproduce the experimentally determined temperature dependence of the rates and KIEs.[17] The weak temperature dependence is due to the small free energy barrier, which arises from a balance between the total reorganization energy and the driving force. The unusually large KIE of 81 at room temperature results from the relatively small overlap of the reactant and product vibrational wave functions and the dominance of the lowest energy reactant and product vibronic states for the tunneling process. Based on the nonadiabatic PCET rate expression in eq 1, the ratio of the rate for hydrogen to that for deuterium is approximately proportional to the ratio of the squares of the couplings, which in turn is approximately proportional to the ratio of the squares of the overlaps depicted in Figure 4. The overlaps decay exponentially as the proton donor–acceptor distance increases, but the overlap for deuterium decays faster than that for hydrogen. As a result, the ratio
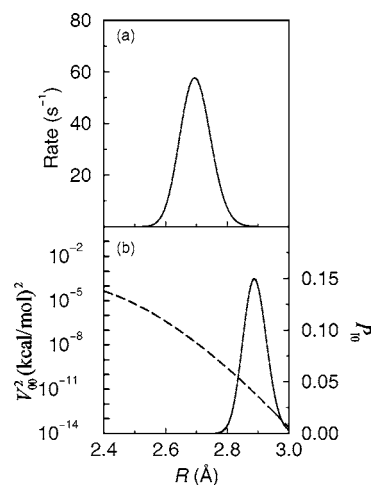

FIGURE 5. Analysis of the dependence of the rate of the PCET reaction catalyzed by SLO on the proton donor–acceptor distance R. Panel a presents the contribution to the overall rate as a function of R. The overall rate is obtained by integration of this function. The dominant contribution to the overall PCET rate corresponds to the distance $R_{dom} = 2.69$ Å. Panel b presents the square of the coupling, V_{00}^2 (dashed), and the Boltzmann probability, P_{I0} (solid), for the lowest energy reactant and product states as functions of R. Reproduced with permission from ref 23. Copyright 2004 American Chemcal Society.

of the overlaps for hydrogen and deuterium increases as the overlap decreases (i.e., as the proton donor–acceptor distance increases).

We also investigated the dependence of the rate on the proton donor–acceptor distance. As shown in Figure 5a, the maximum contribution to the rate occurs at a C–O distance of ∼2.7 Å. Figure 5b indicates that the equilibrium C–O distance is significantly larger than this dominant distance and that the Boltzmann probability at 2.7 Å is extremely small. On the other hand, the coupling between the vibronic states increases dramatically as the C–O distance decreases. The dominant distance is determined by a balance between the larger coupling and the smaller Boltzmann probability as the C–O distance decreases. The rate is dominated by a relatively low-probability C–O distance because of the larger coupling. If the system were frozen, the C–O distance would not be able to decrease enough to allow efficient catalysis. Motion of the enzyme is critical to ensure sampling of these smaller C–O distances.

Thus, our calculations on SLO illustrate that the proton donor–acceptor motion plays a vital role in decreasing the dominant donor–acceptor distance relative to its equilibrium value. We also showed that the quantum mechanical effects of the donor–acceptor motion impact the magnitude of the rate slightly but are not critical for describing the temperature dependence. In general, the magnitude and temperature dependence of the KIE are determined by the dominant donor–acceptor distance, which depends on the structure and motion of the protein, cofactor, and substrate.

Recently we derived PCET rate expressions that include the explicit molecular environment and the dynamical effects of the proton donor–acceptor motion, as well as
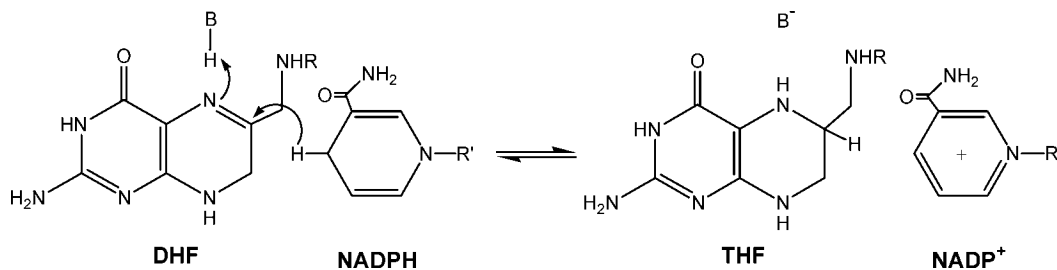
FIGURE 6. The reaction catalyzed by DHFR. The reactant substrate is DHF (dihydrofolate), the product substrate is THF (tetrahydrofolate), and the cofactor is NADPH/NADP$^+$ (nicotinamide adenine dinucleotide phosphate). The calculations focus on the hydride transfer reaction from NADPH to the protonated DHF.

the solvent and enzyme motions.[29] In this approach, the rate constant for nonadiabatic PCET is expressed in terms of a time-dependent probability flux correlation function. We analyzed the dynamical aspects of model PCET reactions in solution with molecular dynamics simulations.[30] The time dependence of the probability flux correlation function is dominated by a solvent damping term, and only the short-time equilibrium fluctuations of the solvent impact the rate. The proton donor–acceptor motion does not impact the dynamical behavior of the reaction but does influence the magnitude of the rate. In the future, this molecular dynamics approach will be utilized to study the detailed mechanism of the PCET reaction catalyzed by SLO.

Dihydrofolate Reductase

Dihydrofolate reductase (DHFR) catalyzes the conversion of dihydrofolate (DHF) to tetrahydrofolate (THF).[31] This enzyme maintains the levels of THF required for the biosynthesis of purines, pyrimidines, and amino acids and is associated with a variety of pharmacological applications. The mechanism of DHFR involves both proton and hydride transfer, as depicted in Figure 6. Our studies have focused on the hydride transfer from the NADPH cofactor to the protonated DHF. This hydride transfer reaction is electronically adiabatic (i.e., occurs on the electronic ground state) due to a large splitting between the ground and excited electronic states. A number of theoretical approaches have been used to study this hydride transfer reaction.[32−42]

We have developed a hybrid quantum/classical molecular dynamics approach for proton and hydride transfer reactions in enzymes.[43] This approach includes electronic and nuclear quantum effects, as well as the motion of the complete solvated enzyme. The electronic quantum effects are included with a two-state EVB potential, where the two states correspond to the hydrogen being bonded to the donor or acceptor. The EVB matrix elements are represented by molecular mechanical terms fit to experimental data. The nuclear quantum effects are included by representing the transferring hydrogen nucleus as a three-dimensional vibrational wave function. This wave function is calculated directly on a grid with a Fourier grid Hamiltonian method[44] for each configuration of the classical nuclei sampled during the molecular dynamics simulations.
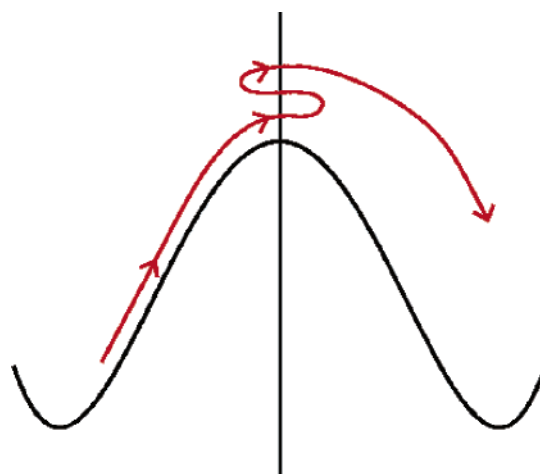

FIGURE 7. Schematic illustration of a free energy profile as a function of a single collective reaction coordinate. The dividing surface is represented by the vertical line passing through the top of the barrier. The trajectory shown exhibits two forward recrossings of the dividing surface. This type of barrier recrossing is a dynamical effect and decreases the transmission coefficient. Reproduced with permission from ref 14. Copyright 2002 American Chemical Society.

The proton or hydride transfer rate constant is given by the simple expression

$$k = \kappa k_{TST} \tag{2}$$

where $k_{TST} = (k_B T/h)\ \exp(-\Delta G^{\dagger}/k_B T)$ is the equilibrium transition state theory rate constant calculated from the activation free energy, $\Delta G^{\dagger}$, and κ is the nonequilibrium transmission coefficient accounting for dynamical recrossings of the barrier. Note that k_{TST} can be expressed in an alternative form that is valid for a general choice of reaction coordinate.[45] Figure 7 provides a schematic depiction of a free energy curve and a trajectory with dynamical barrier recrossings. The activation free energy is obtained from an adiabatic quantum free energy profile, which is generated as a function of a collective reaction coordinate defined to be the difference in energy between the two VB states averaged over the ground state hydrogen vibrational wave function. A series of biasing potentials is used to sample the entire range of the reaction coordinate. The transmission coefficient is calculated with a reactive flux approach,[43,46,47] in which a large number of trajectories are initiated at the top of the barrier and are propagated backward and forward in time. The
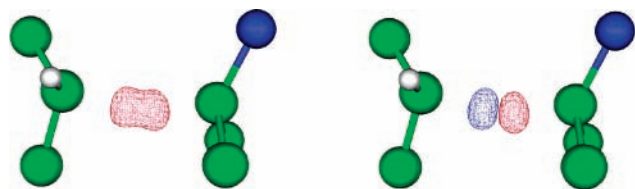
FIGURE 8. Three-dimensional vibrational wave functions representing the transferring hydride for a transition state configuration obtained from simulations of the hydride transfer reaction catalyzed by DHFR. The donor and acceptor carbon atoms and their neighbors are shown. The ground vibrational state is shown on the left, and the excited vibrational state is shown on the right. At the transition state configuration, the hydrogen moves in a virtually symmetric double well potential, so the nuclear wave functions are bilobal and are delocalized between the donor and acceptor. The ground vibrational state is symmetric, and the excited vibrational state is antisymmetric. Reproduced with permission from ref 33. Copyright 2002 American Chemical Society.

molecular dynamics with quantum transitions (MDQT) surface hopping method[5,48] is combined with the reactive flux approach to include vibrationally nonadiabatic effects (i.e., the effects of excited vibrational states).

We have applied this hybrid quantum/classical molecular dynamics approach to the hydride transfer reaction catalyzed by DHFR.[32−34] The two EVB parameters corresponding to the relative energy of and the coupling between the two valence bond states were fit to reproduce the experimental free energies of reaction and activation. Inclusion of the nuclear quantum effects of the transferring hydrogen decreases the free energy barrier by 2.4 kcal/mol.[33] In this framework, the transition state configurations correspond to virtually symmetric double well hydrogen potential energy surfaces, leading to bilobal hydrogen nuclear wave functions delocalized between the hydrogen donor and acceptor. As depicted in Figure 8, the ground vibrational state is symmetric, and the excited vibrational state is antisymmetric for transition state configurations. Analysis of the nuclear wave functions and the splittings between the ground and excited vibrational states for the transition state configurations indicates that hydrogen tunneling plays a significant role in this reaction. The calculated KIE was consistent with the experimental value of 3.[18,33] Note that the KIE can be relatively small even for reactions with significant hydrogen tunneling in the predominantly adiabatic regime. The transmission coefficient was calculated to be $\kappa = 0.88$, indicating that dynamical barrier recrossings occur but do not significantly impact the overall rate.[33]

The role of motion in DHFR has been studied with a wide range of experimental and theoretical methods. X-ray crystallographic structures of intermediates along the reaction pathway indicate significant conformational changes during the reaction.[49] NMR experiments have identified dynamic regions throughout the enzyme and imply that these dynamic regions are altered along the reaction pathway.[50] Classical molecular dynamics simulations have provided evidence of correlated and anti-correlated motions in the dynamic regions identified with NMR.[15] Kinetic measurements on single and multiple

mutants indicate that mutations far from the active site can significantly impact the hydride transfer rate.[51] Furthermore, a genomic analysis for sequence conservation across 36 species from *Escherichia coli* to human illustrates that residues both in the active site and distal to the active site are conserved across this wide range of species.[32]

Given this background, we analyzed our hybrid quantum/classical molecular dynamics simulation data to further elucidate the role of motion in DHFR.[32,33] We investigated two different types of effects. The first analysis centered on the equilibrium thermally averaged changes in distances and angles along the collective reaction coordinate. These motions potentially occur on the millisecond time scale of hydride transfer and impact the free energy barrier. In this approach, we performed several nanoseconds of molecular dynamics simulations for each biasing potential along the collective reaction coordinate, and the data from the different biasing potentials were combined to generate the entire free energy profile for the chemical reaction. Assuming adequate equilibration for each biasing potential, this procedure provides information about the equilibrium motions occurring on the experimentally determined millisecond time scale of hydride transfer. Recently, protein motions on this time scale have been observed in single molecule fluorescence experiments.[52] The second analysis centered on the correlation of distances and angles at the transition state to the degree of dynamical barrier recrossing. These motions occur on the femtosecond to picosecond time scale and impact the transmission coefficient. Since the transmission coefficient is a prefactor in the rate expression, whereas the free energy barrier is in the exponential, motions that impact the free energy barrier will typically have a greater effect on the overall rate.

This analysis resulted in the identification and characterization of a network of coupled motions in DHFR.[32,33] These equilibrium, thermally averaged motions are located throughout the enzyme, spanning the active site and the exterior. These motions represent conformational changes along the collective reaction coordinate corresponding to reorganization of the environment to facilitate hydride transfer by bringing the donor and acceptor closer, orienting the substrate and cofactor properly, and providing a favorable electrostatic environment. We emphasize that these motions are not *dynamically* coupled to the chemical reaction but rather represent equilibrium conformational changes that enable hydride transfer.

To further elucidate this network of coupled motions, we analyzed changes in the structure, hydrogen bonding, and electrostatics along the collective reaction coordinate.[34] Analysis of the thermally averaged reactant, transition state, and product structures indicates that the key features of the enzyme structure are retained throughout the reaction, but significant structural differences are apparent in the loop regions. Moreover, a number of hydrogen bonds are broken and formed throughout the enzyme during the reaction. Analysis of the electrostatic potential for the thermally averaged reactant, transition state, and product structures implies that this potential
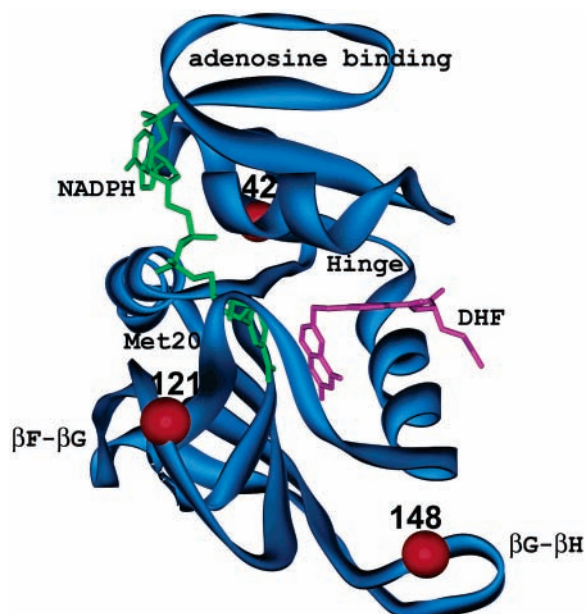
FIGURE 9. Three-dimensional structure of wild-type DHFR with the NADPH cofactor shown in green and the DHF substrate shown in magenta. The important loop regions are identified, and the residues involved in the mutant DHFR enzymes studied are labeled with red spheres.[36]

FIGURE 10. Three-dimensional structure of wild-type DHFR with the NADPH cofactor shown in green and the DHF substrate shown in magenta. Residues 17 and 37 are labeled with red spheres. In the constrained simulations, the distance between the α-carbons of these two residues is fixed.[37]

changes dramatically during the reaction, even in regions far from the active site. The electrostatic contributions from a number of residues distal to the active site were found to change significantly during the reaction. This detailed analysis illustrates that the rather subtle conformational changes occurring during the hydride transfer reaction substantially alter the hydrogen bonding and electrostatics throughout the entire enzyme.

We also performed hybrid quantum/classical molecular dynamics simulations for the G121V mutant DHFR enzyme.[35] As depicted in Figure 9, this residue is on the exterior of the enzyme and is located more than 12 Å from the active site. Nevertheless, kinetic experiments showed that mutation of residue 121 from glycine to valine decreased the rate of hydride transfer by a factor of 163.[51,53] We mutated this residue to valine and followed the same procedure with the identical EVB parameters used for the wild-type DHFR simulations. The calculated free energy barrier was 3.4 kcal/mol greater for the mutant than for the wild-type enzyme. This increase in the barrier is consistent with the experimental observation of a decrease in the rate by a factor of 163, which corresponds to ~3.0 kcal/mol increase in the free energy barrier when the effects of the transmission coefficient are neglected. We found that the transmission coefficient is not significantly altered by the mutation. Analysis of the thermally averaged structural properties along the collective reaction coordinate indicates that some of the motions correlated to hydride transfer in the wild-type enzyme are attenuated or absent in the mutant. These results suggest that this distal mutation interrupts the network of coupled motions, thereby decreasing the probability of sampling configurations conducive to hydride transfer and increasing the free energy barrier.
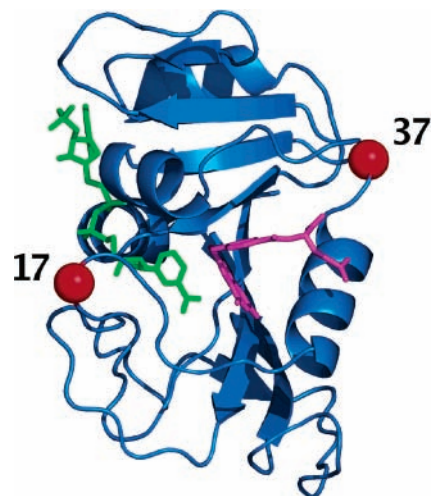
After this initial study, we performed simulations for the triple mutant M42F−G121S−S148A and the corresponding single and double mutants.[36] The locations of these distal residues are depicted in Figure 9. Kinetic experiments indicate that these distal mutations significantly decrease the rate of hydride transfer and that some of these mutations are nonadditive (i.e., the change in the free energy barrier for the multiple mutation is not equal to the sum of the changes for the single mutations). We analyzed these mutants with a rank correlation analysis method, which compares thermally averaged changes along the collective reaction coordinate to a specified target model.[36] This analysis was performed for all interatomic distances in the system comprised of the enzyme, cofactor, and substrate. The results illustrate that residues throughout the enzyme participate in the network of coupled motions correlated to hydride transfer and that each mutant samples a unique distribution of motions. The observation of nonadditive changes to the network of coupled motions provides an explanation for the experimentally observed nonadditivity of the rates. This study provides further validation that distal mutations can lead to nonlocal structural changes[54] and significantly impact the probability of sampling conformations conducive to hydride transfer.[39,40]

Recently we performed hybrid quantum/classical molecular dynamics simulations in which a single constraint was applied to the distance between the α-carbons of residues 17 and 37, as illustrated in Figure 10.[37] The constrained residues are on the exterior of the enzyme and are separated by ~28 Å. The choice of this constraint was motivated by recent single molecule experiments, in which residues 17 and 37 were labeled with fluorescent probes.[52] The overall activity and hydride transfer rates were not altered by the presence of the probes. The fluorescence resonance energy transfer (FRET) was analyzed using single molecule fluorescence microscopy

under equilibrium conditions for hydride transfer. The experimental data indicate motion between residues 17 and 37 on a similar time scale as that of the hydride transfer reaction. Our simulations of DHFR without the constraint predicted a change of ~0.5 Å in the thermally averaged equilibrium distance between the α-carbons of residues 17 and 37 during hydride transfer.[34] We found that constraining the distance between these distal residues increased the free energy barrier for hydride transfer by ~3 kcal/mol.[37] These simulations suggest that freezing a single motion between distal residues alters the network of coupled motions and the conformational sampling of the entire system enough to significantly impact the rate of hydride transfer.

Conclusions

Hydrogen tunneling is significant in the reactions catalyzed by both SLO and DHFR. SLO catalyzes a nonadiabatic PCET reaction involving two distinct electronic states, whereas DHFR catalyzes a predominantly adiabatic hydride transfer reaction occurring on a single electronic state. The rate expression for nonadiabatic PCET reactions is based on the Golden rule, which requires relatively small couplings between the reactant and product vibronic states. In this case, the hydrogen tunnels between two different electronic states. The rate expression for predominantly adiabatic proton and hydride transfer reactions is based on transition state theory with corrections for dynamical barrier recrossings. In this case, the hydrogen tunnels on a single electronic surface.

Protein motion also plays an important role in the reactions catalyzed by SLO and DHFR. For both reactions, a decrease of the proton donor−acceptor distance relative to its equilibrium value is required to enable efficient hydrogen tunneling. In both cases, equilibrium thermal motions of the protein strongly impact the reaction, but the dynamical aspects of these motions are not critical. The fast femtosecond to picosecond thermal fluctuations of the protein lead to conformational changes on the slower millisecond time scale of the reaction. These equilibrium conformational changes are averaged over the faster thermal fluctuations and facilitate hydrogen transfer by bringing the donor and acceptor closer, orienting the substrate and cofactor optimally, and providing a favorable electrostatic environment. In DHFR, we have identified and characterized a network of coupled motions corresponding to these conformational changes. Distal mutations were found to interrupt this network of coupled motions through nonlocal structural changes and to alter the conformational sampling of the entire enzyme. This analysis provides an explanation for the experimentally observed impact of distal mutations on the hydride transfer rate, as well as the nonadditive effects of multiple mutations.

The importance of hydrogen tunneling and protein motion in enzyme reactions has implications for protein engineering and drug design. Mutation of distal residues could impact the structure and conformational sampling

of the entire enzyme and thus alter the free energy barrier, as well as the probability of hydrogen tunneling. The interplay between theory and experiment will continue to aid in the elucidation of the fundamental principles underlying these types of enzyme reactions. The long-term objective is to develop methodology to design enzymes with specified properties and characteristics.

References

(1) Garcia-Viloca, M.; Gao, J.; Karplus, M.; Truhlar, D. G. How enzymes work: Analysis by modern rate theory and computer simulations. *Science* **2004**, *303*, 186−195.
(2) Benkovic, S. J.; Hammes-Schiffer, S. A perspective on enzyme catalysis. *Science* **2003**, *301*, 1196−1202.
(3) Warshel, A. *Computer Modeling of Chemical Reactions in Enzymes and Solutions*; John Wiley & Sons: New York, 1991.
(4) Azzouz, H.; Borgis, D. A quantum molecular dynamics study of proton-transfer reactions along asymmetrical H-bonds in solution. *J. Chem. Phys.* **1993**, *98*, 7361−7375.
(5) Hammes-Schiffer, S.; Tully, J. C. Proton transfer in solution: Molecular dynamics with quantum transitions. *J. Chem. Phys.* **1994**, *101*, 4657−4667.
(6) Kiefer, P. M.; Hynes, J. T. Nonlinear free energy relations for adiabatic proton-transfer reactions in a polar environment. II. Inclusion of the hydrogen bond vibration. *J. Phys. Chem. A* **2002**, *106*, 1850−1861.
(7) Borgis, D.; Hynes, J. T. Dynamical theory of proton tunneling transfer rates in solution: general formulation. *Chem. Phys.* **1993**, *170*, 315−346.
(8) Cui, Q.; Karplus, M. Promoting modes and demoting modes in enzyme-catalyzed proton-transfer reactions: A study of models and realistic systems. *J. Phys. Chem. B* **2002**, *106*, 7927−7947.
(9) Antoniou, D.; Caratzoulas, S.; Kalyanaraman, C.; Mincer, J. S.; Schwartz, S. D. Barrier passage and protein dynamics in enzymatically catalyzed reactions. *Eur. J. Biochem.* **2002**, *269*, 3103−3112.
(10) Klinman, J. P. Dynamic barriers and tunneling. New views of hydrogen transfer in enzyme reactions. *Pure Appl. Chem.* **2003**, *75*, 601−608.
(11) Sutcliffe, M. J.; Scrutton, N. S. A new conceptual framework for enzyme catalysis. *Eur. J. Biochem.* **2002**, *269*, 3096−3102.
(12) Gao, J. Catalysis by enzyme conformational change as illustrated by orotidine 5′-monophosphate decarboxylase. *Curr. Opin. Struct. Biol.* **2003**, *13*, 184−192.
(13) Kohen, A.; Cannio, R.; Bartolucci, S.; Klinman, J. P. Enzyme dynamics and hydrogen tunnelling in a thermophilic alcohol dehydrogenase. *Nature* **1999**, *399*, 496−499.
(14) Hammes-Schiffer, S. Impact of enzyme motion on activity. *Biochemistry* **2002**, *41*, 13335−13343.
(15) Radkiewicz, J. L.; Brooks, C. L. Protein dynamics in enzymatic catalysis: Exploration of dihydrofolate reductase. *J. Am. Chem. Soc.* **2000**, *122*, 225−231.
(16) Sikorski, R. S.; Wang, L.; Markham, K. A.; Rajagopalan, P. T. R.; Benkovic, S. J.; Kohen, A. Tunneling and coupled motion in the *Escherichia coli* dihydrofolate reductase catalysis. *J. Am. Chem. Soc.* **2004**, *126*, 4778−4779.
(17) Knapp, M. J.; Rickert, K. W.; Klinman, J. P. Temperature-dependent isotope effects in soybean lipoxygenase-1: Correlating hydrogen tunneling with protein dynamics. *J. Am. Chem. Soc.* **2002**, *124*, 3865−3874.
(18) Fierke, C. A.; Johnson, K. A.; Benkovic, S. J. Construction and evaluation of the kinetic scheme associated with dihydrofolate reductase from *Escherichia coli*. *Biochemistry* **1987**, *26*, 4085−4092.
(19) Samuelsson, B.; Dahlen, S.-E.; Lindgren, J.; Rouzer, C. A.; Serhan, C. N. Leukotrienes and lipoxins: structures, biosynthesis, and biological effects. *Science* **1987**, *237*, 1171−1176.
(20) Cukier, R. I.; Nocera, D. G. Proton-coupled electron transfer. *Annu. Rev. Phys. Chem.* **1998**, *49*, 337−369.
(21) Mayer, J. M. Proton-coupled electron transfer: A reaction chemist's view. *Annu. Rev. Phys. Chem.* **2004**, *55*, 363−390.

(22) Lehnert, N.; Solomon, E. L. Density-functional investigation on the mechanism of H-atom abstraction by lipoxygenase. *J. Biol. Inorg. Chem.* **2003**, *8*, 294−305.

(23) Hatcher, E.; Soudackov, A. V.; Hammes-Schiffer, S. Proton-coupled electron transfer in soybean lipoxygenase. *J. Am. Chem. Soc.* **2004**, *126*, 5763−5775.

(24) Olsson, M. H. M.; Siegbahn, P. E. M.; Warshel, A. Simulations of the Large Kinetic Isotope Effect and the Temperature Dependence of the Hydrogen Atom Transfer in Lipoxygenase. *J. Am. Chem. Soc.* **2004**, *126*, 2820−2828.

(25) Siebrand, W.; Smedarchina, Z. Temperature dependence of kinetic isotope effects for enzymatic carbon−hydrogen bond cleavage. *J. Phys. Chem. B* **2004**, *108*, 4185−4195.

(26) Soudackov, A.; Hammes-Schiffer, S. Multistate continuum theory for multiple charge transfer reactions in solution. *J. Chem. Phys.* **1999**, *111*, 4672−4687.

(27) Soudackov, A.; Hammes-Schiffer, S. Derivation of rate expressions for nonadiabatic proton-coupled electron transfer reactions in solution. *J. Chem. Phys.* **2000**, *113*, 2385−2396.

(28) Hammes-Schiffer, S.; Iordanova, N. Theoretical studies of proton-coupled electron transfer reactions. *Biochim. Biophys. Acta−Bioenerg.* **2004**, *1655*, 29−36.

(29) Soudackov, A.; Hatcher, E.; Hammes-Schiffer, S. Quantum and dynamical effects of proton donor−acceptor vibrational motion in nonadiabatic proton-coupled electron transfer reactions. *J. Chem. Phys.* **2005**, *122*, No. 014505.

(30) Hatcher, E.; Soudackov, A.; Hammes-Schiffer, S. Comparison of dynamical aspects of electron, proton, and proton-coupled electron transfer reactions. *Chem. Phys.*, in press.

(31) Miller, G. P.; Benkovic, S. J. Stretching exercises − flexibility in dihydrofolate reductase catalysis. *Chem. Biol.* **1998**, *5*, R105−R113.

(32) Agarwal, P. K.; Billeter, S. R.; Rajagopalan, P. T. R.; Benkovic, S. J.; Hammes-Schiffer, S. Network of coupled promoting motions in enzyme catalysis. *Proc. Natl. Acad. Sci. U.S.A.* **2002**, *99*, 2794−2799.

(33) Agarwal, P. K.; Billeter, S. R.; Hammes-Schiffer, S. Nuclear quantum effects and enzyme dynamics in dihydrofolate reductase catalysis. *J. Phys. Chem. B* **2002**, *106*, 3283−3293.

(34) Wong, K. F.; Watney, J. B.; Hammes-Schiffer, S. Analysis of electrostatics and correlated motions for hydride transfer in dihydrofolate reductase. *J. Phys. Chem. B* **2004**, *108*, 12231−12241.

(35) Watney, J. B.; Agarwal, P. K.; Hammes-Schiffer, S. Effect of mutation on enzyme motion in dihydrofolate reductase. *J. Am. Chem. Soc.* **2003**, *125*, 3745−3750.

(36) Wong, K. F.; Selzer, T.; Benkovic, S. J.; Hammes-Schiffer, S. Impact of distal mutations on the network of coupled motions correlated to hydride transfer in dihydrofolate reductase. *Proc. Nat. Acad. Sci. U.S.A.* **2005**, *102*, 6807−6812.

(37) Sergi, A.; Watney, J. B.; Wong, K. F.; Hammes-Schiffer, S. Freezing a single distal motion in dihydrofolate reductase. *J. Am. Chem. Soc.*, submitted for publication.

(38) Garcia-Viloca, M.; Truhlar, D. G.; Gao, J. Reaction-path energetics and kinetics of the hydride transfer reaction catalyzed by dihydrofolate reductase. *Biochemistry* **2003**, *42*, 13558−13575.

(39) Thorpe, I. F.; Brooks, C. L., III Barriers to hydride transfer in wild type and mutant dihydrofolate reductase from *E. coli*. *J. Phys. Chem. B* **2003**, *107*, 14042−14051.

(40) Thorpe, I. F.; Brooks, C. L, III The coupling of structural fluctuations to hydride transfer in dihydrofolate reductase. *Proteins: Struct., Funct,, Bioinformatics* **2004**, *57*, 444−457.

(41) Castillo, R.; Andres, J.; Moliner, V. Catalytic mechanism of dihydrofolate reductase enzyme: A combined quantum-mechanical/molecular mechanical characterization of transition state structure for the hydride transfer step. *J. Am. Chem. Soc.* **1999**, *121*, 12140−12147.

(42) Cummins, P. L.; Greatbanks, S. P.; Rendell, A. P.; Gready, J. E. Computational methods for the study of enzymic reaction mechanisms 1. Application to the hydride transfer step in the catalysis of dihydrofolate reductase. *J. Phys. Chem. B* **2002**, *106*, 9934−9944.

(43) Billeter, S. R.; Webb, S. P.; Iordanov, T.; Agarwal, P. K.; Hammes-Schiffer, S. Hybrid approach for including electronic and nuclear quantum effects in molecular dynamics simulations of hydrogen transfer reactions in enzymes. *J. Chem. Phys.* **2001**, *114*, 6925−6936.

(44) Webb, S. P.; Hammes-Schiffer, S. Fourier grid Hamiltonian multiconfigurational self-consistent field: A method to calculate multidimensional hydrogen vibrational wave functions. *J. Chem. Phys.* **2000**, *113*, 5214−5227.

(45) Watney, J. B.; Soudackov, A.; Wong, K. F.; Hammes-Schiffer, S., manuscript in preparation.

(46) Chandler, D. In *Classical and Quantum Dynamics in Condensed Phase Simulations*; Berne, B. J., Ciccotti, G., Coker, D. F., Eds.; World Scientific: Singapore, 1998; pp 3−23.

(47) Neria, E.; Karplus, M. A position dependent friction model for solution reactions in the high friction regime: Proton transfer in triosephosphate isomerase (TIM). *J. Chem. Phys.* **1996**, *105*, 10812−10818.

(48) Tully, J. C. Molecular dynamics with electronic transitions. *J. Chem. Phys.* **1990**, *93*, 1061−1071.

(49) Sawaya, M. R.; Kraut, J. Loop and subdomain movements in the mechanism of *Escherichia coli* dihydrofolate reductase: Crystallographic evidence. *Biochemistry* **1997**, *36*, 586−603.

(50) Osborne, M. J.; Schnell, J.; Benkovic, S. J.; Dyson, H. J.; Wright, P. E. Backbone dynamics in dihydrofolate reductase complexes: Role of loop flexibility in the catalytic mechanism. *Biochemistry* **2001**, *40*, 9846−9859.

(51) Rajagopalan, P. T. R.; Lutz, S.; Benkovic, S. J. Coupling interactions of distal residues enhance dihydrofolate reductase catalysis: Mutational effects on hydride transfer rates. *Biochemistry* **2002**, *41*, 12618−12628.

(52) Hammes, G. G.; Benkovic, S. J. Private communication.

(53) Cameron, C. E.; Benkovic, S. J. Evidence for a functional role of the dynamics of glycine-121 of *Escherichia coli* dihydrofolate reductase obtained from kinetic analysis of a site-directed mutant. *Biochemistry* **1997**, *36*, 15792−15800.

(54) Swanwick, R. S.; Shrimpton, P. J.; Allemann, R. K. Pivotal role of Gly 121 in dihydrofolate reductase from *Escherichia coli*: The altered structure of a mutant enzyme may form the basis of its diminished catalytic performance. *Biochemistry* **2004**, *43*, 4119−4127.